Supporting Information

Raman Spectra and Strain Effects in Bismuth Oxychalcogenides

Ting Cheng, [†,‡] Congwei Tan, [†,‡] Shuqing Zhang, [£] Teng Tu, [†]

Hailin Peng, [†,‡,§,*] and Zhirong Liu[†,‡,§,*]

[†] College of Chemistry and Molecular Engineering, Peking University, Beijing 100871, China.

[‡] Center for Nanochemistry, Academy for Advanced Interdisciplinary Studies, Peking University, Beijing 100871, China

[£] The Low-Dimensional Materials and Devices Laboratory, Tsinghua-Berkeley Shenzhen Institute, Tsinghua University, Shenzhen 518055, Guangdong, China

[§] State Key Laboratory for Structural Chemistry of Unstable and Stable Species, Beijing National Laboratory for Molecular Sciences, Peking University, Beijing 100871, China

[*] Address correspondence to hlpeng@pku.edu.cn and LiuZhiRong@pku.edu.cn

1. SEM images of the sample

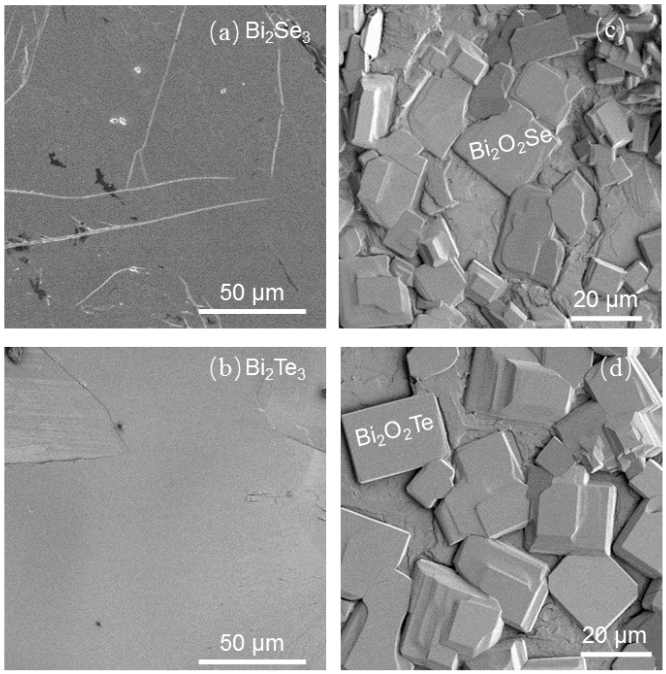

Figure S1. SEM images of bulk (a) Bi_2Se_3, (b) Bi_2Te_3 and CVD-grown (c) Bi_2O_2Se, (d) Bi_2O_2Te. It can be seen an obvious phase transformation from Bi_2Se_3 (Bi_2Te_3) to Bi_2O_2Se (Bi_2O_2Te).

2. The calculated Band structure using the LDA method.

Limited by our server computing performance and low calculation efficiency of MBJ or HSE method in Quantum-Espresso package, we just do the band calculation using the LDA method in Quantum-Espresso package and to have a qualitative understanding of band dispersion. And also compare the dispersion with the results using the PBE-MBJ method implemented in VASP along the same high-symmetry path in the Brillouin zone to verify the electron density.

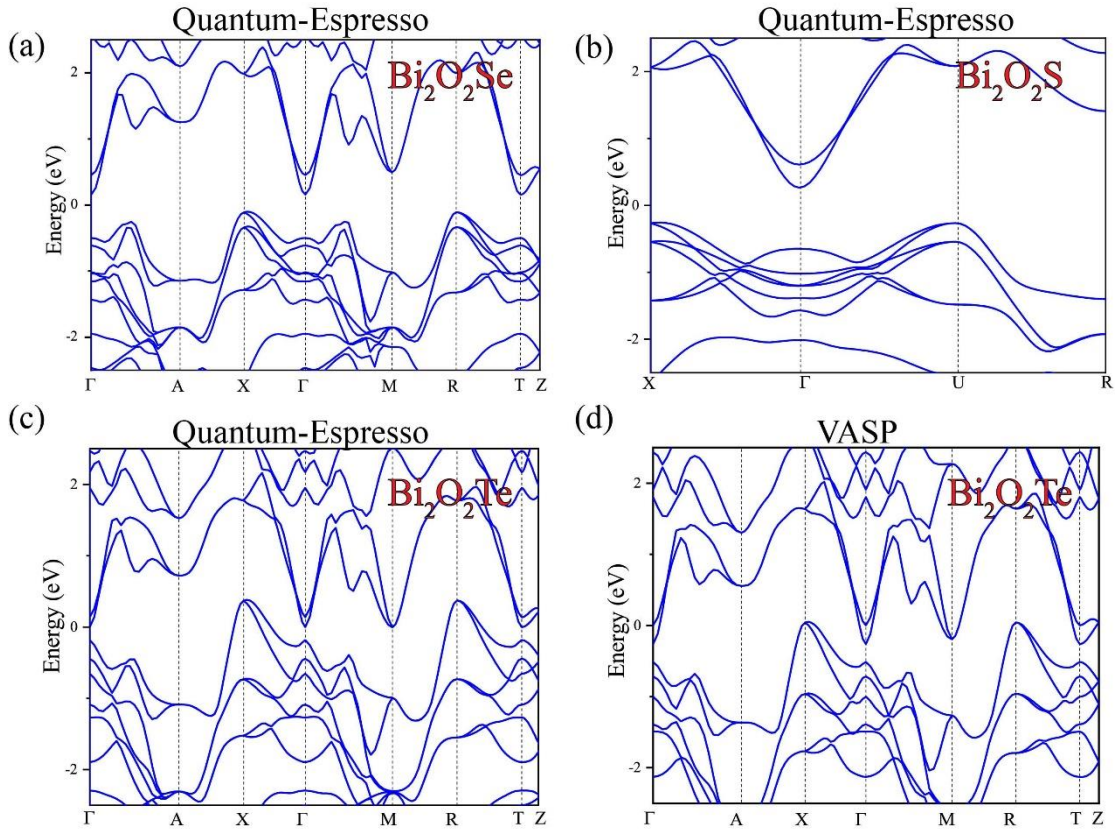

Figure S2. Electronic band structures of (a) Bi_2O_2Se, (b) Bi_2O_2S, (c) Bi_2O_2Te calculated by LDA method using the Quantum Espresso package, and (d) Bi_2O_2Te calculated by LDA method using the VASP. SOC effect was considered here.

3. The Calculated atomic displacements for all remaining Raman-active modes in Bi_2O_2S (D_{2h} symmetry).

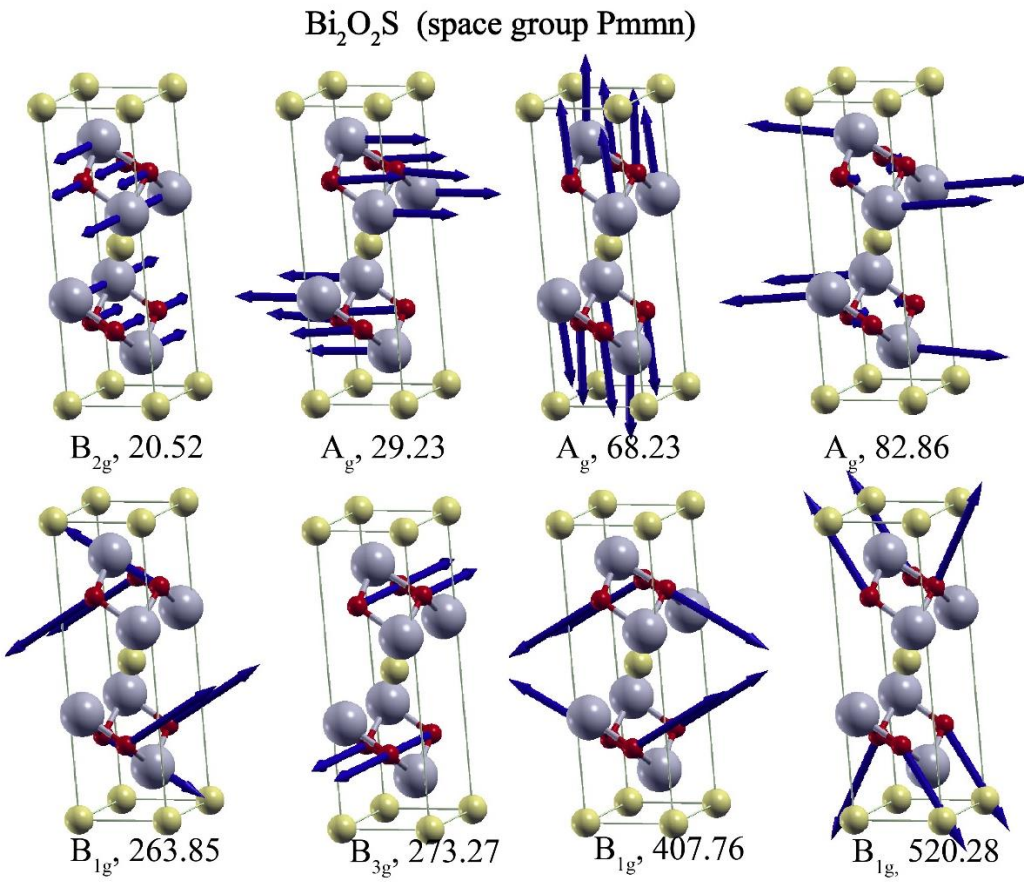

Figure S3. The calculated polarization vectors of all Raman-active modes in Bi_2O_2S except the modes which have been shown in the main paper.

4. Separate the A_{1g} and B_{1g} mode in theory

Considering the light polarization configuration, $\boldsymbol{e}_i$ and $\boldsymbol{e}_s$ are the polarization vectors of the incoming and scattered photons, respectively. Selection rules help us to know that the intensity of the A_{1g} mode is independent of the sample orientation, but the B_{1g} mode is strongly related ($I_{B1g}(\theta) \sim c^2\sin^2(\theta+2\beta)$, where $\theta = \angle(\boldsymbol{e}_i, \boldsymbol{e}_s)$, $\beta = \angle(\boldsymbol{e}_i, \boldsymbol{x})$). The diagram illustration was shown in Figure S3 (a). Figure S3 (b) gives the intensity of the A_{1g} and B_{1g} modes as a function of the crystal orientation with respect to the laboratory axes $\boldsymbol{x}_0$ and $\boldsymbol{y}_0$.

It can be seen that, in the parallel polarization configuration (θ=0°), the intensity of B_{1g} mode is maximal when the orientation of the sample is parallel to $\boldsymbol{e}_i$ (β=0°), then gradually decreases to zero for β =45°. But the A_{1g} always keeps constant when the orientation of the sample changes. In the crossed polarization configuration (θ=90°), the intensity of B_{1g} mode gradually increases from zero (β =0°) to its maximal value for β =45°, whereas A_{1g} mode vanishes in this configuration. So we could choose specified sample orientation (β=45°, x'=1/√2[110], y'=1/√2[1-10]) and various polarized scattering configuration to assign four different modes in the Bi_2O_2Se (Bi_2O_2Te) system (see Figure S3 (c)). This hypothesis could be verified by future polarized Raman scattering experiments when obtain a good sample.

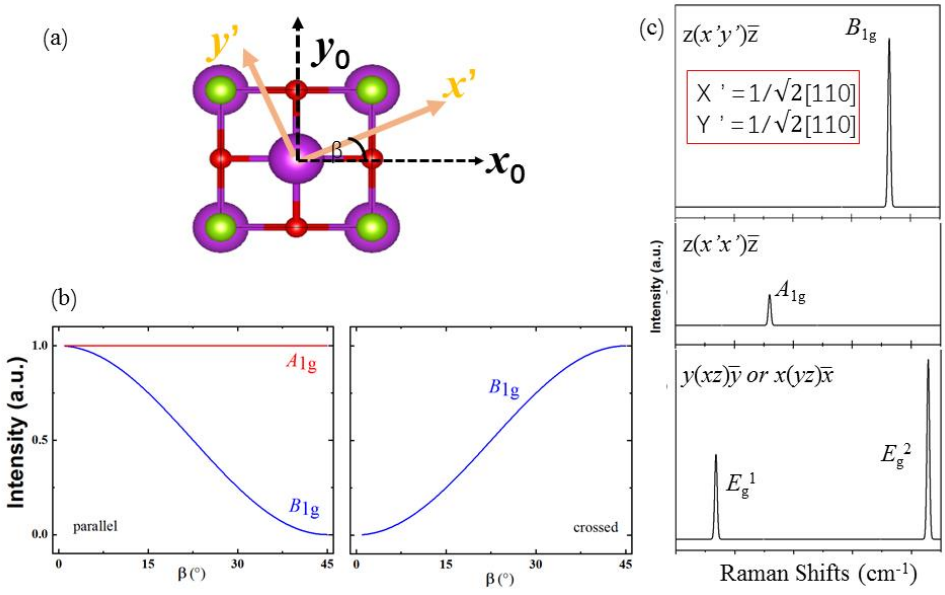

Figure S4. (a) The Scheme for considering the sample orientation β with respect to the laboratory axes $\boldsymbol{x}_0$ and $\boldsymbol{y}_0$. (b) variation of the intensities I [A_{1g}] and I [B_{1g}] versus sample orientation β in the parallel and crossed polarization configurations. (c) the predicted polarized Raman scattering spectra of Bi2O2Se (Bi2O2Te) in various scattering configurations ($\boldsymbol{x}$ = [110], $\boldsymbol{y}$ = [010], x'=1/√2[110], y'=1/√2[1-10], z = [001]).

5. Detailed process for deducing the frequency response functions with small strains

For degenerate modes, it will split into two modes under uniaxial strain. Therefore, we could suppose the Hamiltonian with the energies of two modes as the eigenvalues has such form:

$$H = \begin{bmatrix} a & c \\ c & b \end{bmatrix} \tag{S1}$$

where a, b and c are matrix elements. The solutions of Eq. (S1) are:

$$\omega_{1,2} = \frac{(a+b) \pm \sqrt{(a-b)^2 + 4c^2}}{2} \tag{S2}$$

The two frequency modes degeneracy conditions are: a=b and c=0. Under small strains, we could suppose that the parameter a, b and c expands like:

$$\begin{cases} a = a_0 + \alpha_1 \varepsilon_{xx} + \beta_1 \varepsilon_{yy} + \chi_1 \gamma \\ b = a_0 + \alpha_2 \varepsilon_{xx} + \beta_2 \varepsilon_{yy} + \chi_2 \gamma \\ c = c_0 + \alpha_3 \varepsilon_{xx} + \beta_3 \varepsilon_{yy} + \chi_3 \gamma \end{cases} \tag{S3}$$

To substitute Eq. (S3) into Eq. (S2), we could have:

$$\begin{aligned} \omega_{1,2} = a_0 + & \frac{(\alpha_1 + \alpha_2)\varepsilon_{xx} + (\beta_1 + \beta_2)\varepsilon_{yy} + (\chi_1 + \chi_2)\gamma}{2} \\ & \pm \frac{\sqrt{[(\alpha_1 - \alpha_2)\varepsilon_{xx} + (\beta_1 - \beta_2)\varepsilon_{yy} + (\chi_1 - \chi_2)\gamma]^2 + 4(\alpha_3 \varepsilon_{xx} + \beta_3 \varepsilon_{yy} + \chi_3 \gamma)^2}}{2} \end{aligned} \tag{S4}$$

Then we could simplify Eq. (S4) by symmetry restrictions of the D_{4h} point group:

(1) Inversion operation: to change the sign of shear strain ($\gamma \rightarrow -\gamma$), the symmetry is not broken. That is:

$$\begin{aligned}\omega_{1,2} &= a_0 + \frac{(\alpha_1+\alpha_2)\varepsilon_{xx} + (\beta_1+\beta_2)\varepsilon_{yy} + (\chi_1+\chi_2)\gamma}{2} \\ &\pm \frac{\sqrt{[(\alpha_1-\alpha_2)\varepsilon_{xx} + (\beta_1-\beta_2)\varepsilon_{yy} + (\chi_1-\chi_2)\gamma]^2 + 4(\alpha_3\varepsilon_{xx} + \beta_3\varepsilon_{yy} + \chi_3\gamma)^2}}{2} \\ &\equiv a_0 + \frac{(\alpha_1+\alpha_2)\varepsilon_{xx} + (\beta_1+\beta_2)\varepsilon_{yy} - (\chi_1+\chi_2)\gamma}{2} \\ &\pm \frac{\sqrt{[(\alpha_1-\alpha_2)\varepsilon_{xx} + (\beta_1-\beta_2)\varepsilon_{yy} - (\chi_1-\chi_2)\gamma]^2 + 4(\alpha_3\varepsilon_{xx} + \beta_3\varepsilon_{yy} - \chi_3\gamma)^2}}{2}\end{aligned} \tag{S5}$$

Thus we have

$$\begin{cases}\chi_1 + \chi_2 = 0 \\ (\alpha_1-\alpha_2)(\chi_1-\chi_2) + 4\alpha_3\chi_3 = 0 \\ (\beta_1-\beta_2)(\chi_1-\chi_2) + 4\beta_3\chi_3 = 0\end{cases} \tag{S6}$$

(2) Isotropic system: to apply the biaxial strain ($\varepsilon_{xx}=\varepsilon_{yy}=\varepsilon$, $\gamma=0$), the symmetry is conserved and no split happens. That is:

$$\frac{\sqrt{[(\alpha_1-\alpha_2)\varepsilon + (\beta_1-\beta_2)\varepsilon]^2 + 4(\alpha_3\varepsilon + \beta_3\varepsilon)^2}}{2} \equiv 0 \tag{S7}$$

Thus, we have

$$\begin{cases}\alpha_1 + \beta_1 = \alpha_2 + \beta_2 \\ \alpha_3 + \beta_3 = 0\end{cases} \tag{S8}$$

(3) The system is conserved after a rotation of 90°: At this time, the strain after rotation will be:

$$\begin{aligned}\begin{bmatrix}\varepsilon_{xx}' & \gamma' \\ 0 & \varepsilon_{yy}'\end{bmatrix} &= \begin{bmatrix}\cos\theta & \sin\theta \\ -\sin\theta & \cos\theta\end{bmatrix}\begin{bmatrix}\varepsilon_x' & \gamma' \\ 0 & \varepsilon_y'\end{bmatrix}\begin{bmatrix}\cos\theta & -\sin\theta \\ \sin\theta & \cos\theta\end{bmatrix} \\ &= \begin{bmatrix}\varepsilon_{yy} & 0 \\ -\gamma & \varepsilon_{xx}\end{bmatrix}\end{aligned} \tag{S9}$$

Then,

$$\omega_{1,2} = a_0 + \frac{(\alpha_1+\alpha_2)\varepsilon_{xx} + (\beta_1+\beta_2)\varepsilon_{yy} + (\chi_1+\chi_2)\gamma}{2} \pm \frac{\sqrt{[(\alpha_1-\alpha_2)\varepsilon_{xx} + (\beta_1-\beta_2)\varepsilon_{yy} + (\chi_1-\chi_2)\gamma]^2 + 4(\alpha_3\varepsilon_{xx} + \beta_3\varepsilon_{yy} + \chi_3\gamma)^2}}{2}$$
$$\equiv a_0 + \frac{(\alpha_1+\alpha_2)\varepsilon_{yy} + (\beta_1+\beta_2)\varepsilon_{xx} - (\chi_1+\chi_2)\gamma}{2} \pm \frac{\sqrt{[(\alpha_1-\alpha_2)\varepsilon_{yy} + (\beta_1-\beta_2)\varepsilon_{xx} - (\chi_1-\chi_2)\gamma]^2 + 4(\alpha_3\varepsilon_{yy} + \beta_3\varepsilon_{xx} - \chi_3\gamma)^2}}{2}$$

Based on Eq. (8), we have:

$$\alpha_1 + \alpha_2 = \beta_1 + \beta_2 \tag{S10}$$

In all, we substitute Eq. (S6), (S8) and (S10) into the initial Eq. (S4), the frequencies of degenerate mode under small strain will be:

$$\begin{aligned}\omega_{1,2} &= \omega_0 + \frac{(\alpha_1+\alpha_2)}{2}(\varepsilon_{xx}+\varepsilon_{yy}) \pm \frac{\sqrt{\left[(\alpha_1-\alpha_2)(\varepsilon_{xx}-\varepsilon_{yy}) + 2\chi_1\gamma\right]^2 + 4[\alpha_3(\varepsilon_{xx}-\varepsilon_{yy}) + \chi_3\gamma]^2}}{2} \\ &= \omega_0 + \frac{(\alpha_1+\alpha_2)}{2}(\varepsilon_{xx}+\varepsilon_{yy}) \pm \frac{\sqrt{[(\alpha_1-\alpha_2)^2 + 4\alpha_3^2](\varepsilon_{xx}-\varepsilon_{yy})^2 + 4(\chi_1^2+\chi_3^2)\gamma^2}}{2}\end{aligned} \tag{S11}$$

Define $\bar{k} = \frac{\alpha_1+\alpha_2}{2}, \Delta k = \sqrt{\frac{1}{4}(\alpha_1-\alpha_2)^2 + \alpha_3^2}; k_\gamma = \sqrt{\chi_1^2+\chi_3^2}$, we could further simplify Eq. (S11) as:

$$\omega_{1,2}(\varepsilon_{xx}, \varepsilon_{yy}, \gamma) = \omega_0 + \bar{k}(\varepsilon_{xx}+\varepsilon_{yy}) \pm \sqrt{[\Delta k(\varepsilon_{xx}-\varepsilon_{yy})]^2 + (k_\gamma\gamma)^2} \tag{S12}$$

This gives a universal formula between small strains and frequencies of the split doubly degenerate modes for D_{4h} symmetry systems.

6. Calculated 2D elastic constant evaluation for monolayer Bi_2O_2Se and Bi_2O_2Te.

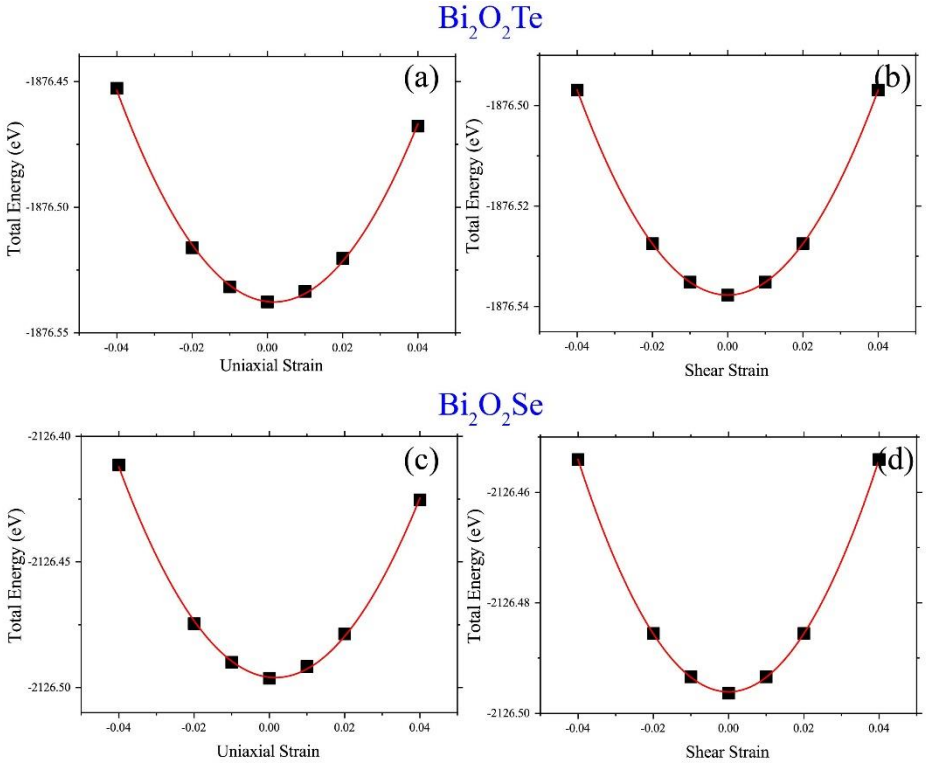

Figure S5. 2D elastic constant evaluation (Total energy with respect to the uniaxial strain and shear strain) for the (a, b) Bi_2O_2Te and (c, d) Bi_2O_2Se. The quadratic fit gives the 2D elastic constant.

7. The remaining evolutions of all Raman modes with small strains (both uniaxial and shear strains) for bulk and monolayer Bi_2O_2Se (Bi_2O_2Te).

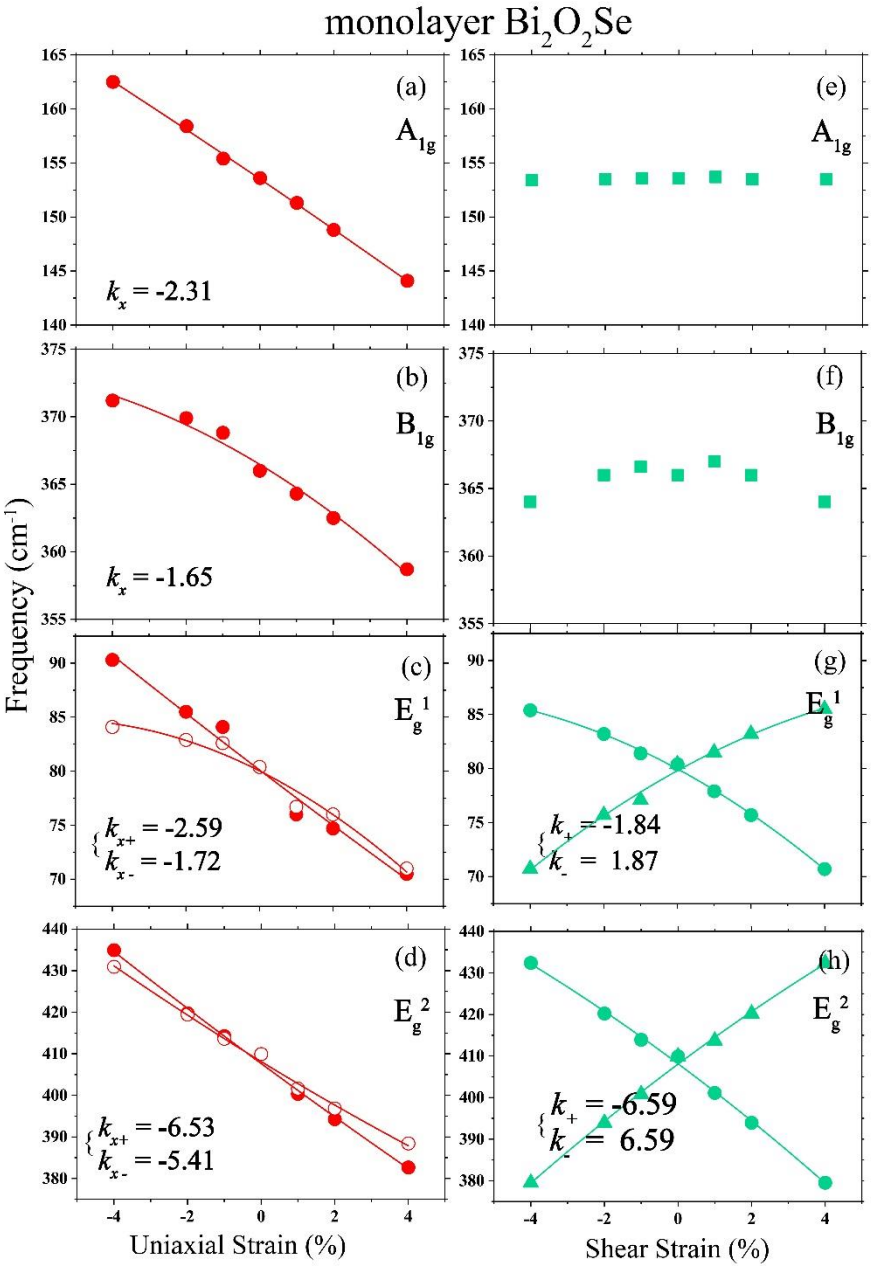

Figure S6. The evolutions of Raman shift with (a-d) uniaxial and (e-h) shear strain along the *x* direction for monolayer Bi_2O_2Se. The calculated data points (squares and triangles) are fitted with a parabolic equation (solid lines) and the fitted linear coefficients (unit: $cm^{-1}/\%$) are also shown in the panels. For the degenerate modes, the open and filled symbols are used to distinguish the two splitting frequencies under the uniaxial strain.

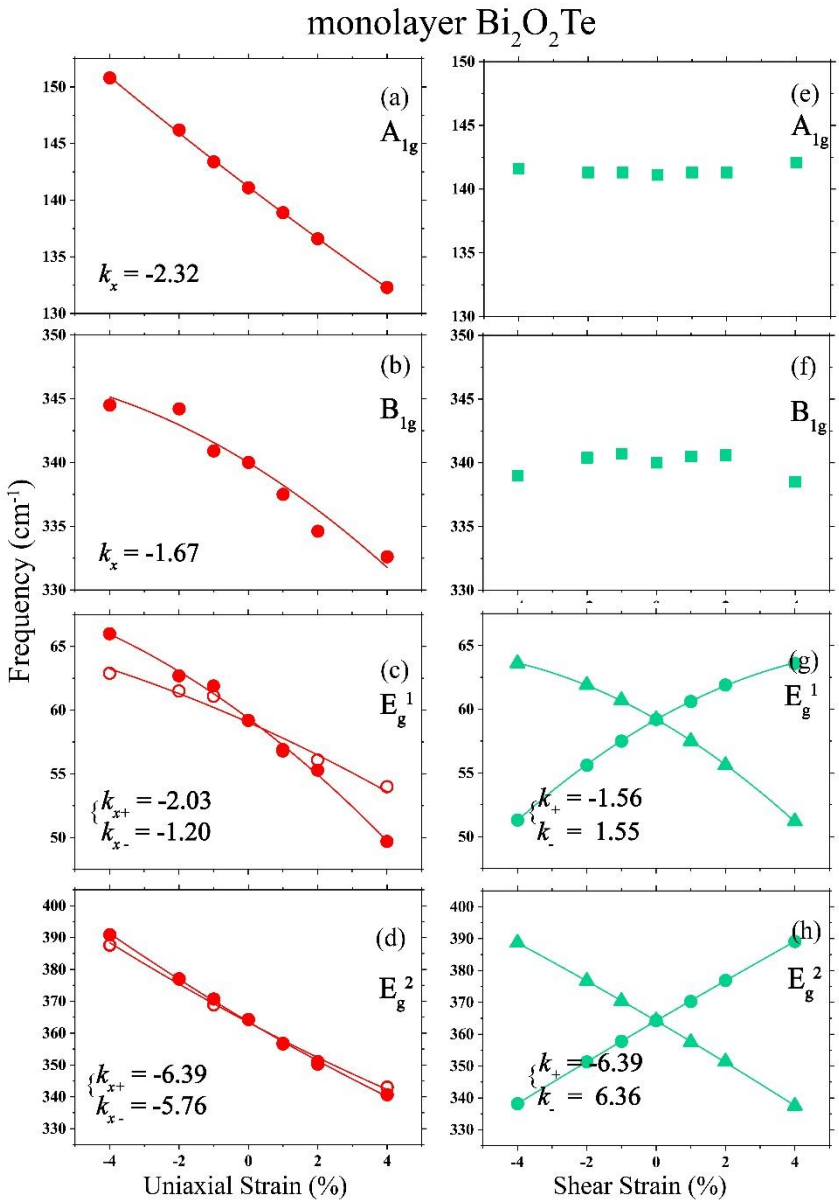

Figure S7. The evolutions of Raman shift with (a-d) uniaxial and (e-h) shear strain along the *x* direction for monolayer Bi_2O_2Te. The calculated data points (squares and triangles) are fitted with a parabolic equation (solid lines) and the fitted linear coefficients (unit: $cm^{-1}/\%$) are also shown in the panels. For the degenerate modes, the open and filled symbols are used to distinguish the two splitting frequencies under the uniaxial strain.

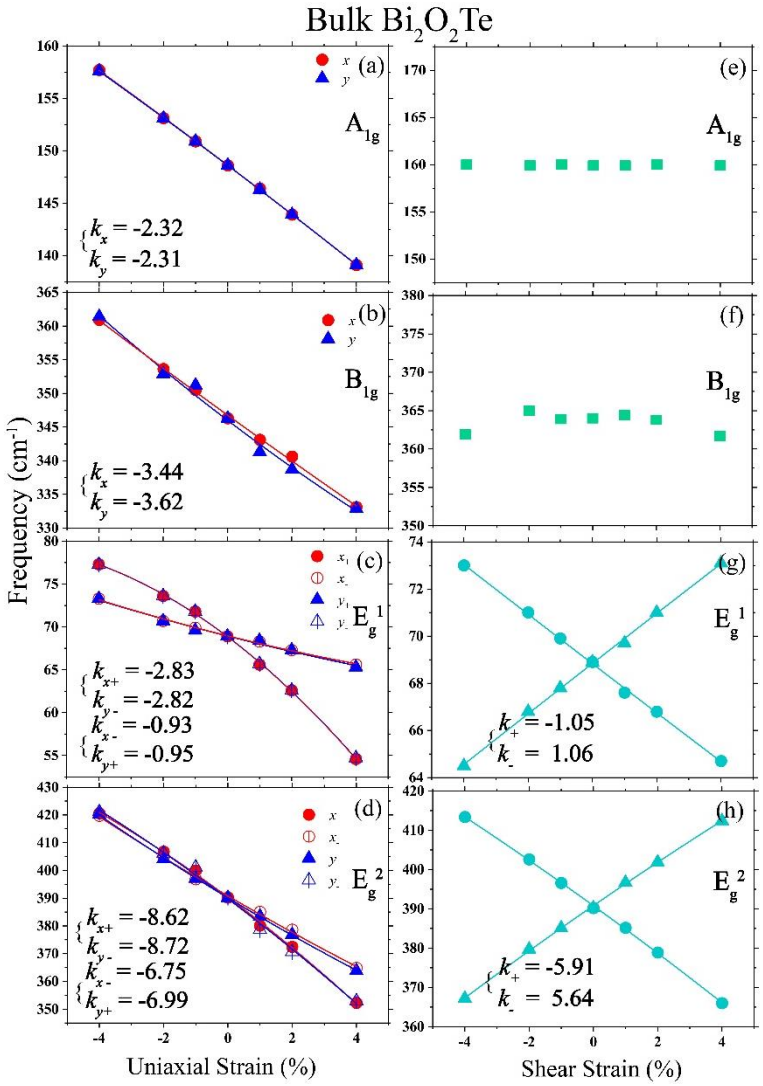

Figure S8. The evolutions of Raman shift with (a-d) uniaxial and (e-h) shear strain along the *x* direction for bulk Bi_2O_2Te. The calculated data points (squares and triangles) are fitted with a parabolic equation (solid lines) and the fitted linear coefficients (unit: $cm^{-1}/\%$) are also shown in the panels. For the degenerate modes, the open and filled symbols are used to distinguish the two splitting frequencies under the uniaxial strain.

Table S1. Determined slopes for four Raman-active modes in bulk and monolayer Bi_2O_2Se and Bi_2O_2Te under applied strain ε_{xx} and γ.

Slope k	Bi_2O_2Se				Bi_2O_2Te			
	Bulk		Monolayer		Bulk		Monolayer	
	k_{xx}	k_γ	k_{xx}	k_γ	k_{xx}	k_γ	k_{xx}	k_γ
E_g^1	-2.37; -0.66	-0.81; 0.81	-2.59; -1.72	-1.84; 1.87	-2.83; -0.93	-1.05; 1.06	-2.03; -1.20	-1.56; 1.55
A_{1g}	-2.32	0	-2.31	0	-2.32	0	-2.32	0
B_{1g}	-3.00	0	-1.65	0	-3.44	0	-1.67	0
E_g^2	-8.47; -6.97	-6.36; 6.29	-6.53; -5.41	-6.59; 6.59	-8.62; -6.75	-5.91; 5.64	-6.39; -5.76	-6.39; 6.36

8. The corresponding θ-dependent frequency change of the degenerate modes in monolayer and bulk Bi_2O_2Se (Bi_2O_2Te).

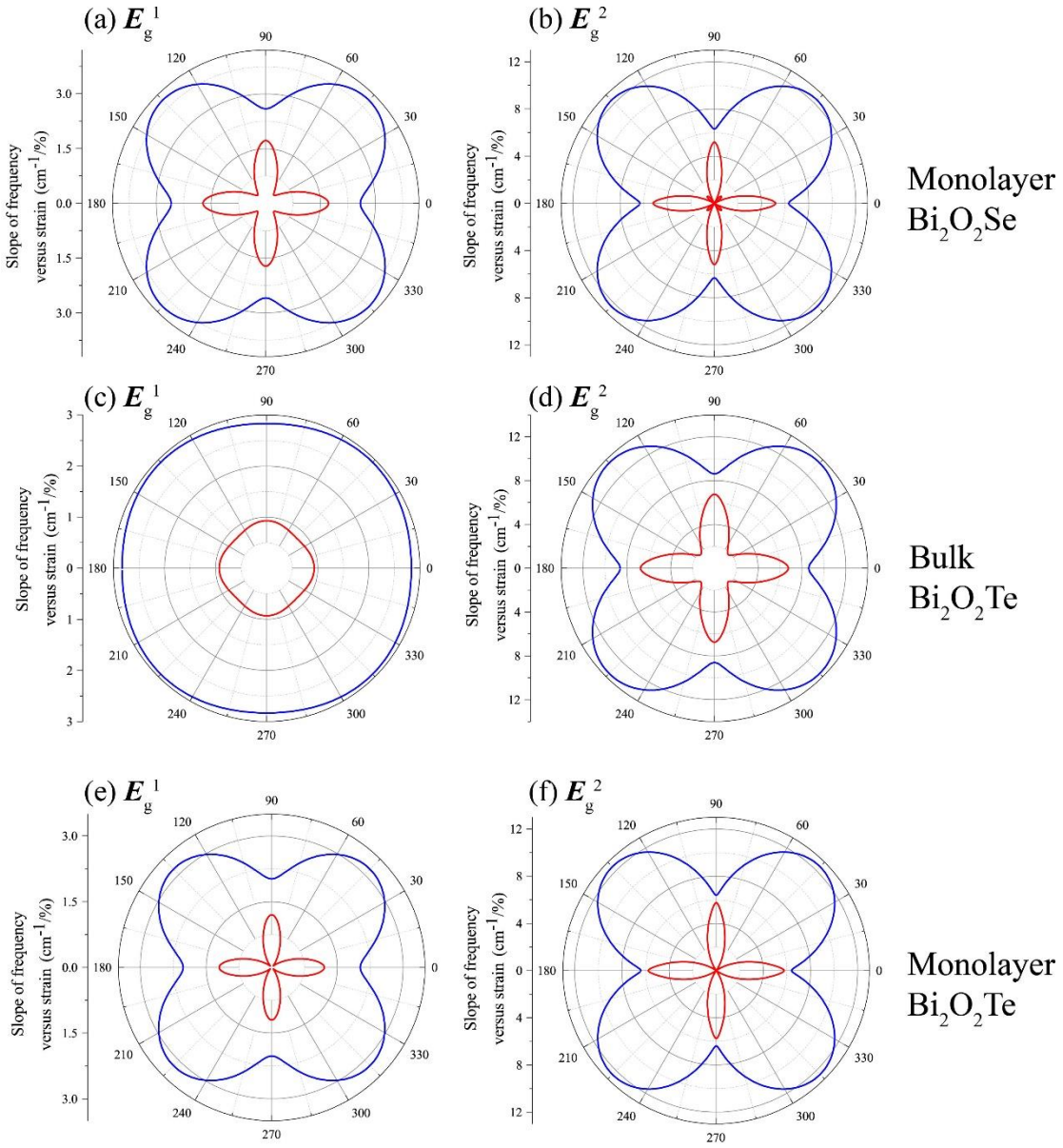

Figure S9. The corresponding θ-dependent frequency change of degenerate modes in (a-b) monolayer Bi_2O_2Se, (c-d) bulk Bi_2O_2Te and (e-f) monolayer Bi_2O_2Te.